Available online at www.sciencedirect.com
SCIENCE DIRECT®
Thermochimica Acta 409 (2004) 25–32
thermochimica acta
www.elsevier.com/locate/tca

Concentration dependencies of NaCl salting of lysozyme by calorimetric methods

Jarosław Poznański, Małgorzata Wszelaka-Rylik, Wojciech Zielenkiewicz*

Institute of Physical Chemistry, Polish Academy of Sciences, Kasprzaka 44/52, 01-224 Warsaw, Poland

Received 24 March 2003; received in revised form 30 May 2003; accepted 3 June 2003

Abstract

Concentration dependence of NaCl salting of lysozyme was investigated in the range of 0.5–9 mM lysozyme concentration in 0.1 M sodium acetate buffer, pH = 4.25and the concentration of NaCl up to 0.1 M. Calorimetric experiments were performed with the use of a titration ITC Omega MicroCal calorimeter. It was found that the estimated number of bonding sites depended on the lysozyme concentration. For infinitely diluted lysozyme solution, the number of binding sites could be roughly estimated to ∼50. In the range of 2–9 mM protein concentration, the number of weakly binding ($K = 2.7 \pm 0.8\,M^{-1}$) sites on the protein surface was estimated to 35 ± 7. McMillan and Mayer's approach reduced to the third order virial coefficients demonstrates that besides the dominating effect of the protein—salt interaction (a_{11}) the coefficient describing the lysozyme aggregation upon salt addition (a_{12}) is statistically significant.

Keywords: Lysozyme; Salt binding; Titration calorimetry; Virial coefficients

1. Introduction

Hen–egg white lysozyme is a common model system for investigation of the process of macromolecule crystallization. It has been widely used for more than decade as a model of protein crystal growth, and finally it was concluded that protein crystallization is not much different from that of inorganic compounds (for a review see [1]). The interpretation of protein nucleation kinetics in the terms of the protein supersaturated solution non-ideality [2,3] allowed to identify fractal-like aggregates as probable morphological instabilities during crystal growth [4,5]. The idea of fractal aggregates organization was then confirmed by time-resolved dynamic light scattering (DLS) experiments, which proved the existence of oligomers and larger clusters in supersaturated lysozyme solutions [6–9]. The observed nucleation kinetics deviations can be attributed to variations of the initial experimental conditions such as temperature, pH, polydispersity and even the origin of lysozyme [10–12]. The most dominant factors influencing kinetics of lysozyme nucleation are salt composition and both protein and salt concentrations [13]. The high resolution crystallographic structures of hen–egg white lysozyme in the triclinic [14], monoclinic [15], orthotombic [16] and tetragonal [17–20] crystal forms demonstrate the existence of up to eight weakly bound chloride anions [19]. The lysozyme was proved to bind 21–23 chloride anions per molecule in the saturated solution in a sodium acetate/NaCl buffer [21]. Recently, systematic investigations on the chloride anion occupancy in the protein crystals demonstrated that halide anions exhibited ability to relatively non-specific partial substitution of water molecules within the ordered protein solvation shell [22]. In order to enrich knowledge of the salting of the lysozyme we have decided to perform a systematic study of thermodynamic properties of the binding of a chloride anion to the lysozyme in unsaturated solution by the use of an isothermal titration microcalorimeter ITC MicroCal.

2. Experimental

The lysozyme sample (catalog number 629970) purchased from Sigma Chemical Co. (Deisenhofen, Germany) was

* Corresponding author. Tel.: +48-22-632-43-89; fax: +48-22-632-52-76.
E-mail addresses: zivf@ichf.edu.pl (W. Zielenkiewicz), jarek@ibb.waw.pl (J. Poznański).

0040-6031/$ – see front matter © 2003 Elsevier B.V. All rights reserved.
doi:10.1016/S0040-6031(03)00329-0

three times crystallized, dialyzed against water, lyophilized and stored at 4 °C. All experiments were performed in a buffer containing 0.1 M sodium acetate, pH = 4.25.

The calorimetric experiments were performed with the use of a titration ITC Omega MicroCal microcalorimeter. The 0.6 M solution of NaCl was injected in small volumes of 20 μl from a 250 μl injection syringe into a sample cell in a series of 12 controlled pulses to the final concentration of 0.1 M in a sample cell of the volume 1.3611 cm^3. The experiments were made in the conditions when the sample cell at the start of each experiment contained the solution lysozyme in 0.1 M sodium acetate buffer whereas the reference cell was filled with the buffer.

3. Numerical methods

The experimental data obtained from the calorimetric titration were analyzed on the basis of the model of a single set of identical sites (ITC Tutorial Guide). The association equilibrium is expressed in the form:

$$K = \frac{\Theta}{(1-\Theta)[X]} \tag{1}$$

where K is the binding constant, $[X]$ is concentration of free ligand, and Θ is a fraction of sites occupied by ligand X. The total concentration of the ligand X_t is a sum of bulk and free partition expressed in the form

$$X_t = [X] + n\Theta M_t \tag{2}$$

where M_t is a total concentration of macromolecules, n is a number of binding sites, and Θ is a fraction of sites occupied by ligand X. Combining Eqs. (1) and (2) gives

$$\Theta^2 - \Theta\left[1 + \frac{X_t}{nM_t} + \frac{1}{nKM_t}\right] + \frac{X_t}{nM_t} = 0 \tag{3}$$

In principle, the total enthalpy change for the binding (Q) at fractional saturation Θ is

$$Q = n\Theta M_t \,\Delta H\, V_0 \tag{4}$$

where ΔH is the molar heat of a ligand binding and V_0 is an active cell volume. Solving the quadratic Eq. (3) for Q (please note that the second solution has no physical interpretation leading to the fractional saturation (Θ) greater than 1) and then substituting this into Eq. (4) gives

$$Q = \frac{nM_t\,\Delta H\, V_0}{2}\left[1 + \frac{X_t}{nM_t} + \frac{1}{nKM_t} - \sqrt{\left(1 + \frac{X_t}{nM_t} + \frac{1}{nKM_t}\right)^2 - \frac{4X_t}{nM_t}}\right] \tag{5}$$

The theoretical value of Q defined above can be calculated for any designated values of n, K and ΔH and for any solute composition described by M_t and X_t. Lets define $\tilde{Q}(i)$ as the total enthalpy change for the ligand binding calculated, according to Eq. (5), for the macromolecule and ligand concentrations corresponding to the solution composition at the end of the ith injection. The experimentally determined heat released from the ith injection, $\Delta Q^{exp}(i)$, after correction for the solution volume displaced from the sample cell upon injection (dV), could be thus derived from theoretical values, $\tilde{Q}(i)$, as follows:

$$\Delta Q^{exp}(i) = \tilde{Q}(i) + \frac{dV}{V_0}\left[\frac{\tilde{Q}(i) + \tilde{Q}(i-1)}{2}\right] - \tilde{Q}(i-1) \tag{6}$$

where V_0 is the volume of the sample cell.

The process of fitting model (Eq. (5)) to the experimental data, $\Delta Q^{exp}(i)$, through Eq. (6) was carried out with the use of implementation of Marquardt–Levenberg non-linear least-squares algorithm [23] from gnuplot [24].

According to McMillan and Mayer's approach [25] the heat effects have been also analyzed in the terms of virial pairwise coefficients. Calculations were performed by linearization of the model, with the use of an in-home implemented standard regression analysis algorithm in the following form:

$$\tilde{Q}(n) = \sum_{i+j<4; i,j\geq 0} a_{ij}(M_{t,n})^i (X_{t,n})^j \tag{7}$$

where $\tilde{Q}(n)$ is the total heat effect involved in the series of n succeeding injections, $X_{t,n}$ and $M_{t,n}$ are the salt and lysozyme concentrations in the sample cell after n injections. In fact correction for the displaced volumes upon injection was required. Thus, according to Eq. (6) the total heat effect arising from n succeeding injections could be expressed in the form

$$Q^{exp}(n) = \sum_{k=1}^{n} \frac{\Delta Q^{exp}(k)[1 - (dV/2V_0)]^{n-k}}{[1 + (dV/2V_0)]^{n-k+1}} \tag{8}$$

where $\Delta Q^{exp}(k)$ is the experimental integrated heat effect upon the kth injection of a volume dV into the sample cell of a volume V_0. Analogous corrections for the lysozyme and salt concentration were done.

The parameters, a_{ij}, of the model were optimized to minimize the deviations between the estimated enthalpy change upon binding, $\tilde{Q}(n)$, (Eq. (7)) and the experimental derived $Q^{exp}(n)$ (Eq. (8)). The models' quality was analyzed with the Snedecor's F-test [26]. The successive reductions in the number of virial coefficients used in the model were made on the basis of Student's t-statistics [26]. The coefficients with the lowest t-statistics were successively removed from the analysis.

Table 1
The integrated heat effects of each of 12 successive injections, ($Q^{exp}(i)$), obtained for 16 series of lysozyme concentration

Injection no. (i)	Experiment																
	0	1	2	3	4	5	6	7	8	9	10	11	12	13	14	15	16
m_x (mM)		0.50	0.70	0.90	1.39	1.49	1.70	2.10	2.30	2.80	3.50	3.79	5.01	5.70	6.28	7.52	8.95
m_y (M)	0.599	0.599	0.605	0.599	0.605	0.599	0.599	0.605	0.599	0.605	0.600	0.599	0.605	0.605	0.599	0.599	0.599
$-\Delta Q^{exp}(i)$ (mJ)																	
1	−4.07	0.80	1.48	1.51	2.28	2.54	2.78	3.35	3.25	4.03	4.96	5.08	6.02	6.78	6.94	8.19	9.28
2	−4.26	0.84	1.30	1.49	2.14	2.46	2.50	3.04	2.99	3.70	4.46	4.77	5.67	6.54	6.59	7.79	8.90
3	−4.21	0.77	1.20	1.29	1.87	2.24	2.31	2.82	2.94	3.47	4.21	4.70	5.35	6.15	6.49	7.44	8.42
4	−4.18	0.72	1.11	1.34	1.70	1.97	2.06	2.61	2.52	3.15	3.78	4.18	5.04	5.76	6.10	7.02	7.95
5	−4.12	0.70	0.96	1.19	1.55	1.83	1.91	2.36	2.37	2.90	3.49	3.77	4.66	5.28	5.76	6.63	7.49
6	−4.06	0.66	0.90	1.09	1.46	1.69	1.90	2.24	2.10	2.74	3.42	3.56	4.42	5.00	5.41	6.28	7.11
7	−3.95	0.56	0.82	1.07	1.37	1.57	1.53	2.05	2.05	2.49	3.26	3.38	4.10	4.68	5.14	5.97	6.76
8	−3.83	0.50	0.79	0.86	1.28	1.50	1.55	1.92	1.92	2.33	3.10	3.19	3.91	4.41	4.87	5.68	6.41
9	−3.77	0.47	0.76	0.84	1.15	1.36	1.47	1.80	1.80	2.16	2.73	2.97	3.68	4.15	4.62	5.40	6.09
10	−3.67	0.47	0.88	0.82	1.08	1.26	1.38	1.70	1.62	2.03	2.58	2.79	3.48	3.91	4.35	5.13	5.78
11	−3.61	0.45	0.68	0.79	1.06	1.21	1.31	1.65	1.61	1.93	2.45	2.66	3.36	3.72	4.21	4.88	5.53
12	−3.51	0.41	0.59	0.70	0.93	1.16	1.23	1.49	1.52	1.75	2.32	2.51	3.09	3.50	3.98	4.64	5.27

The experimental values are corrected for the heat effect of injection of the identical NaCl solution to a sample cell filled by pure buffer. For the comparison experiment 0 exemplifies the heat effect of salt injection to the pure buffer.

4. Results and discussion

4.1. Calorimetric titration data

Sixteen series of experiments were made, in which the NaCl concentration was practically identical, whereas the lysozyme concentrations varied from 0.5 to 8.95 mM. In each experiment, 12 injections were made. The integrated heats are demonstrated as a function of injection number in Table 1, where m_x is the initial concentration of the lysozyme in the cell and m_y is the concentration of NaCl in the syringe. The integrated heat effects of each injection were corrected by subtraction of the corresponding integrated heat effects of NaCl injection to the pure buffer. The obtained titration plot is shown in Fig. 1. Each peak was integrated to yield the dependence on injection number of the enthalpy of dilution of the solution in the syringe.

4.2. Virial coefficients

The analysis of the obtained experimental data of the heat effect was initially performed in the terms of virial pairwise

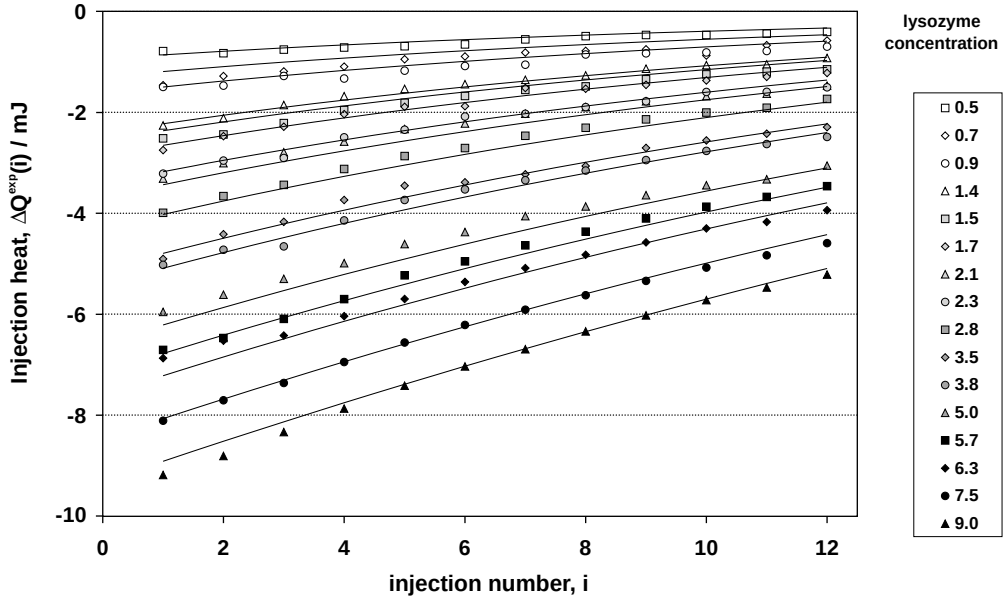

Fig. 1. The titration experiment represented as a function of injection number. The markers correspond to the experimental data. Lines represent fitted model of n independent weakly binding sites on the lysozyme surfaces according to Eq. (6). The parameters of the model correspond to 34 ± 7 binding sites with association constant $2.7 \pm 0.8\,M^{-1}$.

coefficients. It was reduced to the third order coefficients as a result of limiting the model down to three body interactions. The general formula of the equation used was in the form Eq. (7), where the total heat effect ($\tilde{Q}$) arising from mixing solutions of an adequate concentrations of lysozyme and NaCl was corrected for the displaced volumes according to Eq. (8). Optimized parameters a_{ij} are the virial pairwise coefficients. A preliminary analysis performed for the maximal set of 10 coefficients proved that the statistical significance of some coefficients was meaningless. The agreement of the used model with the experimental data was verified with the Fisher test on the basis of the results of linearized regression. In the first stage of the analysis, all the coefficients with Student's *t*-value lower than 2.0 were removed. Upon each next cycle of calculations the parameter with the lowest *t*-value, which is a measure of the coefficient's significance, was removed from the analysis. The optimal set of parameters was chosen as the one for which the Snedecor's *F*-value reached maximum. This procedure led to the reduced set of parameters showing almost unchanged values of both R^2 and standard deviation (S.D. of the fitted surface $\tilde{Q}$([Lys], [NaCl]) from the experimental data) while as a result of the reduced number of parameters the Fisher's *F*-value was significantly increased. The result of the procedure is presented in Table 2.

The highest *F*-value was obtained for four parameter model, but up to two parameter model R^2, S.D. and *F*-values did not vary significantly. Finally, the reduction to the single parameter (a_{11}), coefficient describing lysozyme–salt interaction, was found critical. Despite the fact that the relation $\tilde{Q} = a_{11}$[Lys][NaCl] properly followed the trends observed for the experimental data ($R^2 = 0.977$, $F = 7300$), systematic analysis proved that extension of the set of parameters significantly improves the model quality, which could be analyzed in the terms of either R^2, S.D. or *F*-values. The proposed four parameter model describes the heat effect of (1) lysozyme–salt interaction (a_{11}); (2) lysozyme aggregation upon salt addition (a_{21}); (3) lysozyme dilution upon salt injection (a_{10}) and finally; (4) residual effect of correction for salt dilution upon injection (a_{01}). The stereoview of the fitted and experimental heat effect data as a function of lysozyme and salt concentration is presented in Fig. 2.

The lysozyme–salt interaction was found the most significant participant in the estimated heat effect (50–80%). The correction for the lysozyme dilution varies in the range of 3–6% of the total heat effect while the salt dilution effect does not depend on the lysozyme concentration, and consequently for the most diluted protein solution correction exceeds 50%. The share of a_{21} coefficient for the highest lysozyme concentration reaches up to 35% of the total heat effect.

Finally, it could be concluded that the dominating effect of the lysozyme–salt interaction is accompanied by significant, in the terms of both statistical analysis and estimated share in the total heat effect, salt induced lysozyme aggregation.

4.3. Model of n independent weakly binding sites

The set of integrated experimental heat values, $\Delta Q^{\exp}(i)$, obtained for every injection was analyzed in the terms of *n* binding sites according to Eqs. (5) and (6). Correction for other phenomena but uniform binding was not applied. The results of the analysis of a single experiment consisting of a series of injections to a cell filled with a solution of lysozyme at a given concentration are presented in Table 3. The parameters of the model are strongly correlated (∼0.999), which results in enormously big errors in estimated values. It is evident that, as a result of relatively weak salt binding the titration curves are "flat", what invalidates statistically acceptable analysis of the single experiment. Thus, in the proceeding calculations all the parameters (*n*, *K*, ΔH) were assumed lysozyme concentration independent, and a uniform relation in the form (5), (6) was fitted simultaneously to the set of 16 experimental series. The estimated parameters: $n = (34.5 \pm 7.0)$, $K = (2.7 \pm 0.8)$ M^{-1}, $\Delta H = (-1.7 \pm 0.1)$ kJ/mol are in the range of values obtained for individual series, but the errors are more properly estimated. For the fitted model presented in Fig. 3 root mean square (rms) of residuals equals 1.9 mJ, which significantly exceeds the value obtained for four parameter model based on the virial coefficients (0.7 mJ), but is lower than for a corresponding single parameter model (2.9 mJ).

Analysis of the same model describing the integral heat effect, ($Q^{\exp}(i)$), as a function of injection number, presented in Fig. 1, proves the existence of a number of systematic deviations between the experimental data and the fitted model. Especially for high lysozyme concentration the fitted titration curves are more flat than the experimental data while the opposite tendency is observed for low lysozyme concentration. This clearly indicates that at least one of the *n*, *K*, ΔH parameters from Eq. (5) is an explicit function of the lysozyme concentration.

4.4. Job analysis of the titration experiment

A simple approach to the analysis of titration curves was originally proposed by Job [27]. If the $\tilde{Q}$ is a total heat effect of a salt addition to a final concentration [NaCl] corrected for a displace volume, the value of the [NaCl]$\tilde{Q}$([Lys], [NaCl]) plotted versus partition of NaCl (e.g. [NaCl]/([NaCl] + [Lys]) exhibits maximum, roughly corresponding to the complex stoichiometry. As it is presented in Fig. 4, the position of the maxima changes in the range of 0.85–0.98. This corresponds to the number of binding sites in the range of 6–50, clearly identifying the lysozyme concentration dependence of the binding stoichiometry. For higher concentration stoichiometry is almost constant, while significant decrease of lysozyme concentration (lower value of the effect in Fig. 4) results in strong shift of the maximum towards higher values of stoichiometry.

Table 2
The virial coefficients determined for the salting of lysozyme solutions according to Eq. (6) with the correction for the displaced volume presented in Eq. (7)

Parameter	Number of coefficients applied in the model													
	10		7		5		4		3		2		1	
	Value	*t*-statistics	Value	*t*-statistics	Value	*t*-statistics	Value	*t*-statistics	Value	*t*-statistics	Value	*t*-statistics	Value	*t*-statistics
a_{00} (10^{-4} J)	16 (7)	2.3	6 (3)	1.8										
$-a_{10}$ (10^{-1} J M^{-1})	16 (3)	5.1	15 (3)	5.4	6 (1)	7.3	26 (3)	8.9						
$-a_{01}$ (10^{-2} J M^{-1})	10 (4)	2.5	38 (5)	7.6	39 (3)	15.7	38 (3)	14.6	40 (3)	12.5				
a_{20} (10^{1} J M^{-2})	39 (7)	5.9	33 (7)	4.9	6 (1)	4.6								
$-a_{11}$ (10^{1} J M^{-2})	14 (1)	24.9	13 (1)	41.8	13 (1)	64.2	14 (1)	82.5	14 (1)	70.7	13 (1)	129	13 (1)	139
a_{02} (10^{-1} J M^{-2})	10 (7)	1.4												
$-a_{30}$ (10^{3} J M^{-3})	25 (5)	5.7	20 (5)	4.3										
a_{12} (10^{1} J M^{-3})	5 (4)	1.4												
a_{21} (10^{2} J M^{-3})	28 (4)	7.2	25 (4)	6.6	28 (3)	9.4	38 (2)	18.3	36 (3)	14.5	60 (2)	28.3		
$-a_{03}$ (J M^{-3})	4 (4)	1.1												
F	18159		23468		25655		28734		26313		20762		7301	
R^2	0.9990		0.9988		0.9987		0.9985		0.9978		0.9958		0.9766	
Residuals rms (mJ)	0.60		0.66		0.69		0.73		0.88		1.22		2.87	

Different sets of parameters were used. The reduction of the number of parameters influence both F, R^2 and root of mean square (rms) of residuals.

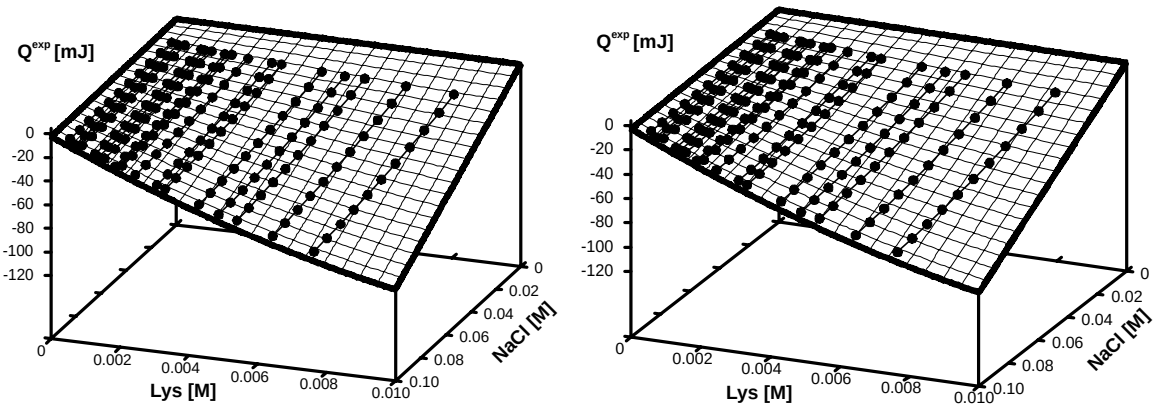

Fig. 2. The titration experiment represented as a function of lysozyme and salt concentration. The circles correspond to the experimental data, thick lines represent successive salt injections in one series, surface represents fitted model of 4 virial coefficients according to Eq. (7) with the correction for displaced volume through Eq. (8). The parameters used: lysozyme–salt interaction (a_{11}); lysozyme aggregation upon salt addition (a_{21}); lysozyme dilution upon salt injection (a_{10}) and residual correction for salt dilution upon injection (a_{01}).

4.5. Model of n concentration dependent weakly binding sites

According to Job's analysis, the titration curve was assumed in the form $Q(n_{\mathrm{Lys}}, K, \Delta H, [\mathrm{Lys}], [\mathrm{NaCl}])$, where K and ΔH values were constrained to the values obtained for the previous model of n independent weakly binding sites, and a number of binding sites n_{Lys} was optimized for each lysozyme concentration separately. Thus, method for treating data permits detailed analysis of the relative changes of number of binding sites in relation to the determined averaged uniform value of 34 ± 7 binding sites. The obtained errors in the range 0.1–0.2 indicated the significance of the concentration dependence of the number of binding sites on the lysozyme surface. The results of the procedure are presented in Fig. 5.

5. Discussion

The interpretation of calorimetric titration experiments demonstrates that lysozyme exhibits ∼35 binding sites with the association constant in the order $1\,\mathrm{M}^{-1}$, which generally agrees with the data obtained with the aid of SPQ fluorescence measurement [21]. Direct analysis as well as Job's model proves that the number of binding sites depends on the lysozyme concentration. Detailed analysis of the calorimetric titration data shows that for lysozyme concentration ranging from 2 to 9 mM in the presence of 100 mM NaCl the number of binding sites remains almost constant (35 ± 1), while decrease of lysozyme concentration results in the significant increase in the number of binding sites. The analysis of statistically most significant virial coefficients strongly suggests that the NaCl induced lysozyme aggregation

Table 3
Evaluated parameters for the model of n independent binding sites, Eqs. (5) and (6), fitted separately to each of 16 series of salt injection experiments

Lysozyme (mM)	N	K (M^{-1})	ΔH_0 ($\mathrm{kJ\,mol}^{-1}$)	rmsd (mJ)
0.5	24.0 ± 2354	1.4 ± 6.6	−1.5 ± 151.6	0.039
0.7	20.0 ± 1272	1.9 ± 8.5	−1.5 ± 99.3	0.096
0.9	20.3 ± 525	1.7 ± 3.6	−1.5 ± 40.9	0.042
1.4	13.1 ± 177	2.4 ± 3.5	−1.5 ± 21.4	0.069
1.5	15.3 ± 155	2.2 ± 2.9	−1.5 ± 16.4	0.064
1.7	14.6 ± 217	2.2 ± 4.4	−1.5 ± 24.1	0.099
2.1	15.6 ± 138	2.0 ± 3.2	−1.5 ± 14.6	0.083
2.3	13.8 ± 133	2.0 ± 3.5	−1.5 ± 16.0	0.090
2.8	13.2 ± 49	2.2 ± 1.8	−1.5 ± 6.3	0.059
3.5	16.8 ± 110	1.7 ± 3.5	−1.5 ± 11.8	0.120
3.8	16.3 ± 82	1.7 ± 3.0	−1.5 ± 9.2	0.110
5.0	19.6 ± 61	1.3 ± 2.1	−1.5 ± 6.3	0.078
5.7	17.3 ± 34	1.5 ± 1.7	−1.5 ± 4.1	0.078
6.3	34.6 ± 82	0.7 ± 2.2	−1.5 ± 7.2	0.069
7.5	30.0 ± 37	0.8 ± 1.6	−1.5 ± 4.1	0.062
9.0	24.9 ± 27	0.9 ± 1.8	−1.5 ± 3.8	0.086

The salt was injected in 12 steps to the cell filled with lysozyme solution at different concentrations.

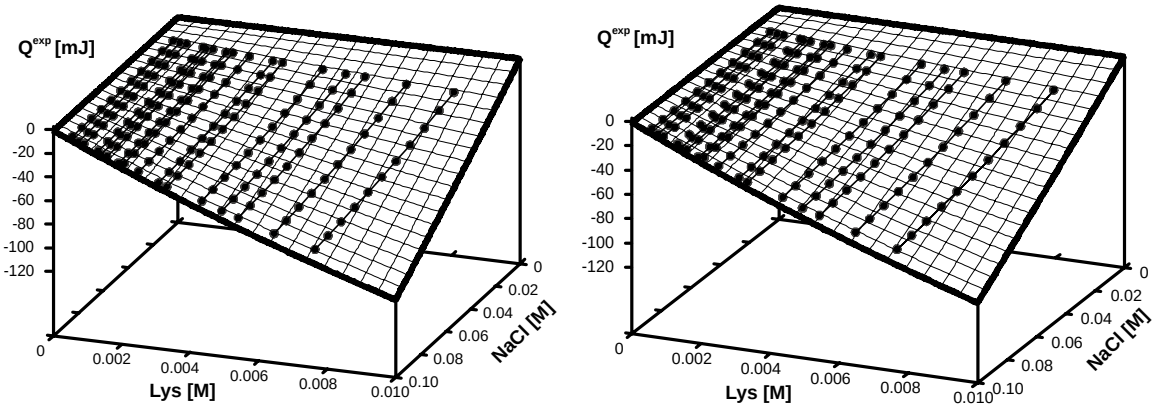

Fig. 3. The titration experiment represented as a function of lysozyme and salt concentration. The circles correspond to the experimental data, thick lines represent successive salt injections in one series, surface represents fitted model of n independent weakly binding sites on the lysozyme surfaces according to Eq. (5) with the correction for the displaced volume through Eq. (6). The parameters of the model correspond to 34 ± 7 binding sites with association constant $2.7 \pm 0.8\,\mathrm{M}^{-1}$.

undergoes even for milimolar concentration of the protein. Thus, aggregation process drives concentration dependence of the number of binding sites on the lysozyme surface. The virial coefficients normalized for the active cell volume and solute density equal $h_x = a_{10} = (-0.11 \pm 0.01)\,\mathrm{kJ\,mol^{-1}}$; $h_{xy} = (1/2)a_{11} = (-2.9 \pm 0.1)\,\mathrm{kJ\,kg\,mol^{-2}}$; $h_{xxy} = (1/3)a_{21} = (43 \pm 3)\,\mathrm{kJ\,kg^2\,mol^{-3}}$, respectively. The enthalpic pairwise interaction coefficients h_{xy} are close to the values determined for NaCl and aqueous solution of a wide spectrum of low mass non-electrolytes lying in the range of $-0.5 \pm 1.2\,\mathrm{kJ\,kg\,mol^{-2}}$ [28,29]. Slightly larger heat effect of NaCl binding by lysozyme is probably correlated with the positive charge carried on the protein surface. At pH 4.25, lysozyme carry 18 positively charged Arg (11), Lys (7) and His (1) groups and nine mostly ionized [30] acidic residues Asp (7) and Glu (2) exhibiting net charge ∼+9. The parameter $a_{01} = (-16 \pm 2)\,\mathrm{J\,mol^{-1}}$ reflects non-ideal correction for the salt dilution upon injection to the cell, and is a measure of the experimental error and cannot be related to heat values of any salt dilutions. The estimated second virial coefficient for lysozyme dilution h_{xx} equals $a_{20} = (2.5 \pm 0.5)\,\mathrm{kJ\,kg\,mol^{-2}}$. The determined weak and non-specific binding of chloride

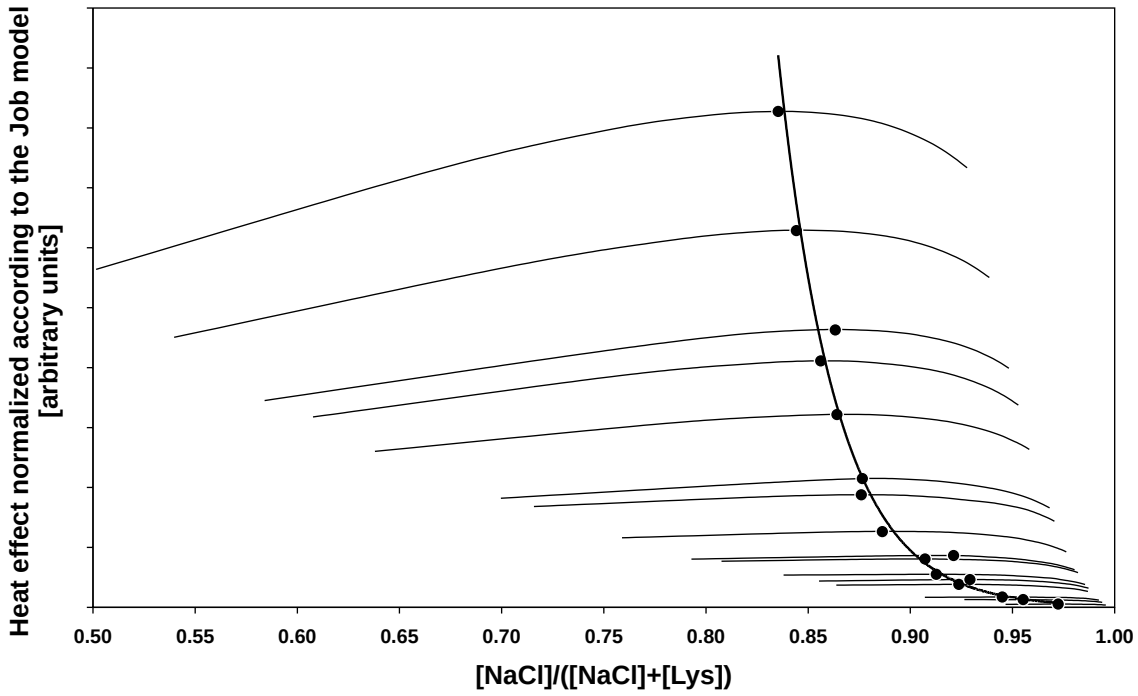

Fig. 4. Stoichiometry of the complexes according to the Job's method. The higher protein concentration corresponds to the larger values of the curve. The maxima, marked by circles, correspond to the estimated salt partition in the complex. The thick line roughly demonstrates concentration dependence of the number of binding sites.

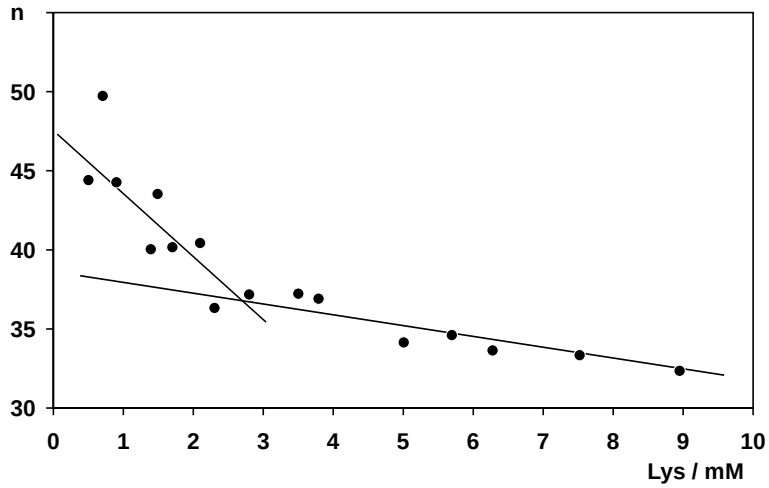

Fig. 5. The estimated number (n) of weakly binding centers on the lysozyme surface as a function of the initial lysozyme concentration in the cell.

anion agrees with the partial occupation of halide anions observed for the short cryo-soaking of protein crystals [22].

Acknowledgements

We gratefully acknowledge the financial support from KBN within the grant No. 7T09A10621.

References

[1] Y. Georgalis, W. Saenger, Curr. Top. Cryst. Growth Res. 4 (1998) 1.
[2] M. Muschol, F. Rosenberger, J. Chem. Phys. 103 (1995) 10424.
[3] M. Muschol, F. Rosenberger, J. Cryst. Growth 167 (1996) 738.
[4] R.F. Xiao, D.J.I. Alexander, F. Rosenberger, Phys. Rev. A38 (1988) 2447.
[5] D.J.I. Alexander, in: J.P. van der Eerden, O.S.L. Bruinsma (Eds.), Science and Technology of Crystal Growth, Lattice Models, Kluwer Academic Publishers, The Netherlands, 1995, pp. 81–95.
[6] S. Tanaka, M. Yamamoto, K. Kawashima, K. Ito, R. Hayagawa, M. Ataka, J. Cryst. Growth 168 (1996) 44.
[7] S. Tanaka, M. Yamamoto, K. Ito, R. Hayagawa, M. Ataka, Phys. Rev. E56 (1997) R67.
[8] W. Eberstein, Y. Georgalis, W. Saenger, J. Cryst. Growth 143 (1994) 71.
[9] Y. Georgalis, P. Umbach, D.M. Soumpasis, W. Saenger, J. Am. Chem. Soc. 121 (1999) 1627.
[10] W. Brown, Dynamic Light Scattering: The Method and Some Applications, Oxford Science Publications, London, 1993.
[11] B.J. Berne, R. Pecora, Dynamic Light Scattering: With Applications to Chemistry, Biology, and Physics, Dover Publications, Dover, 2000.
[12] J. Poznañski, Y. Georgalis, L. Wehr, W. Saenger, P. Zielenkiewicz, Biophys. Chem. 104 (2003) 605.
[13] Y. Georgalis, P. Umbach, A. Zielenkiewicz, E. Utzig, W. Zielenkiewicz, P. Zielenkiewicz, W. Saenger, J. Am. Chem. Soc. 119 (1997) 11959.
[14] M.A. Walsh, T.R. Schneider, L.C. Sieker, Z. Dauter, V.S. Lamzin, K.S. Wilson, Acta Cryst. D54 (1998) 522.
[15] L.K. Steinrauf, Acta Cryst. D54 (1998) 767.
[16] H. Oki, Y. Matsuura, H. Komatsu, A.A. Chernov, Acta Cryst. D55 (1999) 114.
[17] M.C. Vaney, I. Broutin, P. Retailleau, A. Douangamath, S. Lafont, C. Hamiaux, T. Prangé, A. Ducruix, M. Riès-Kautt, Acta Cryst. D57 (2001) 929.
[18] K. Lim, A. Nadarajah, E.L. Forsythe, M.L. Pusey, Acta Cryst. D54 (1998) 899.
[19] M. Dauter, Z. Dauter, E. de la Fortelle, G. Bricogne, G.M. Sheldrick, J. Mol. Biol. 289 (1999) 83.
[20] C. Sauter, F. Otalora, J.A. Gavira, O. Vidal, R. Giege, J.M. Garcia-Ruiz, Acta Cryst. D, Biol. Cryst. D57 (Part 8) (2001) 1119.
[21] L. Sibille, M.L. Pusey, Acta Cryst. D50 (1994) 396.
[22] Z. Dauter, M. Dauter, K.R. Rajashankar, Acta Cryst. D56 (2000) 232.
[23] D.W. Marquardt, J. Soc. Ind. Appl. Math. 11 (1963) 431.
[24] T. Williams, C. Kelley, Gnuplot, Version 3.7, 1998, pp. 1986–1993.
[25] W.G. McMillan, J.E. Mayer, J. Chem. Phys. 13 (1945) 276.
[26] S. Brandt, Data Analysis: Statistical and Computational Methods for Scientists and Engineers with Extensive Source Program Libraries in FORTRAN, third ed. (revised and expanded), Springer, New York, 1999.
[27] P. Job, Ann. Chim. 9 (1928) 113.
[28] H. Piekarski, Can. J. Chem. 64 (1986) 2127.
[29] H. Piekarski, M. Tkaczyk, J. Chem. Soc., Faraday Trans. 87 (1991) 3661.
[30] Y. Y Sham, Z.T. Chu, A. Warshel, J. Phys. Chem. B 101 (1997) 4458.